



# Investigation of a thermoluminescence response and trapping parameters and theoretical model to explain concentration quenching for Yb<sup>3+</sup>-doped ZrO<sub>2</sub> phosphors under UV exposure

KANCHAN UPADHYAY<sup>1</sup>, RAUNAK KUMAR TAMRAKAR<sup>2,\*</sup>  and ANUPAMA ASTHANA<sup>3</sup>

<sup>1</sup>International and Inter University Centre of Nanoscience and Nanotechnology, Mahatma Gandhi University, Kottayam 686560, India

<sup>2</sup>Department of Applied Physics, Bhilai Institute of Technology (Seth Balkrishan Memorial), Near Bhilai House, Durg CG 491001, India

<sup>3</sup>Department of Chemistry, Govt. V Y T PG Autonomous College, Durg 491001, India

\*Author for correspondence (raunak.ruby@gmail.com)

MS received 6 October 2018; accepted 3 January 2019; published online 1 August 2019

**Abstract.** In this paper, a thermoluminescence signal centred at 129°C induced by UV radiation of Yb<sup>3+</sup>-doped ZrO<sub>2</sub> is reported. Phosphor was prepared by a solution combustion method and annealed at 600 and 900°C to study the effect of annealing. The prepared phosphor was characterized by X-ray diffraction and scanning electron microscopy methods. Various parameters were optimized. Computerized glow curve deconvolution was employed and kinetic parameters for every deconvoluted peak were calculated. To understand the concentration quenching, a 3T1R (three trap one recombination centre) model has been proposed.

**Keywords.** Thermoluminescence signal; Yb<sup>3+</sup>-doped ZrO<sub>2</sub>; X-ray diffraction; scanning electron microscopy method; 3T1R model.

## 1. Introduction

Thermoluminescence (TL) is the phenomenon used to measure different kinds of radiation doses. When a phosphor material is exposed to any type of radiation or ultraviolet light, a fraction of free electrons or holes may be trapped by some defects inside the host lattice, known as electron or hole traps. These trapped electrons or holes remain trapped until they obtain enough energy to escape from defect centres. When the provided energy for escaping trapped carriers is thermal energy, then the phenomenon is called TL [1]. For this purpose, many investigations have been conducted. In this sense, oxide-based thermoluminescence dosimetric (TLD) materials have been proposed as a TLD material; there are numerous reports on the dosimetric properties of the oxide-based material as a TL material [2–5].

Out of these oxide materials, zirconia is one of the stable hosts and having an important TL response and it is subjected to UV radiation, gamma and X-rays [6–8]. It has intense TL glow curve with a higher TL signal. This TL signal can be analysed in relation to given doses studied [9]. This oxide-based material has a major disadvantage i.e., it shows an instant loss of the signal within few minutes after exposure to UV radiation [6,7,9]. To overcome this problem, we are using other ions as impurities during the synthesis process to enhance its TL signal [9,10].

The present work demonstrates the synthesis of ZrO<sub>2</sub>:Yb<sup>3+</sup> phosphor by the combustion synthesis method and its structural characterization by X-ray diffraction (XRD), scanning electron microscopy (SEM) and energy-dispersive X-ray (EDX) analyses. The combustion synthesis offers instances with easy experimental arrangement; surprisingly, short time reactions and the easy accessibility of the final phosphor product adapted to synthesize ZrO<sub>2</sub>:Yb<sup>3+</sup> phosphor. The major aim of this work is to study the effect of the addition of Yb<sup>3+</sup> ions to enhance the TL behaviour of the ZrO<sub>2</sub> phosphor material under UV radiation.

## 2. Experimental

The synthesis of ZrO<sub>2</sub>:Yb<sup>3+</sup> (1–10 mol%) by a solution combustion method involves following chemicals as precursor materials, zirconium nitrate (Zr(NO<sub>3</sub>)<sub>3</sub>), ytterbium nitrate (Yb(NO<sub>3</sub>)<sub>3</sub>) (purchased from Sigma Aldrich) and urea used as a fuel. The stoichiometric ratios of an oxidizer and fuel were taken in an alumina crucible to which triple distilled water was added to dissolve the compounds. The redox mixture thus obtained was then introduced into a muffle furnace maintained at 600±10°C. The mixture undergoes dehydration and then decomposes with liberation of large amounts of gases (CO<sub>2</sub> and N<sub>2</sub>). The mixture was then frothed and swelled thus,

forming foam which ruptured with a flame. The whole combustion process was completed in less than a few minutes (<3 min). The Petri dish was taken out from the furnace and a foamy product was crushed into fine powder using a pestle and mortar for 30 min. These powders were calcined at 600–900°C for 1 h, and then subjected to further structural, morphological and luminescence studies [10–12].

### 2.1 Instrument details

The sample was characterized by XRD analysis. XRD data were collected over the range of 20–70° at room temperature. XRD measurements were carried out for all the prepared samples using an X-ray powder diffractometer (Philips make X'Pert PRO Panalytical and Rigaku-miniflex, Japan) with CuK $\alpha$  radiation at a wavelength ( $\lambda$ ) of 1.54 Å, with a voltage

of 40 kV and a current of 30 mA. The Ni filter was used to minimize CuK $\alpha$  radiation. The particle size was calculated using the Scherrer formula. The TL studies were carried out using a TLD reader I1009 supplied by Nucleonix. The sample was irradiated by 254 nm UV radiation. The kinetic parameter was evaluated by Chen's peak shape method and the graph was plotted using Origin 8.0 programme.

## 3. Results and discussion

### 3.1 Structural characterization

Figure 1 shows the XRD pattern of the freshly prepared ZrO<sub>2</sub>:Yb<sup>3+</sup> and annealed phosphor samples. There is a clear broadening of the diffracted peaks, which is due to the nano-range crystal size. The broadening width of the peak decreases

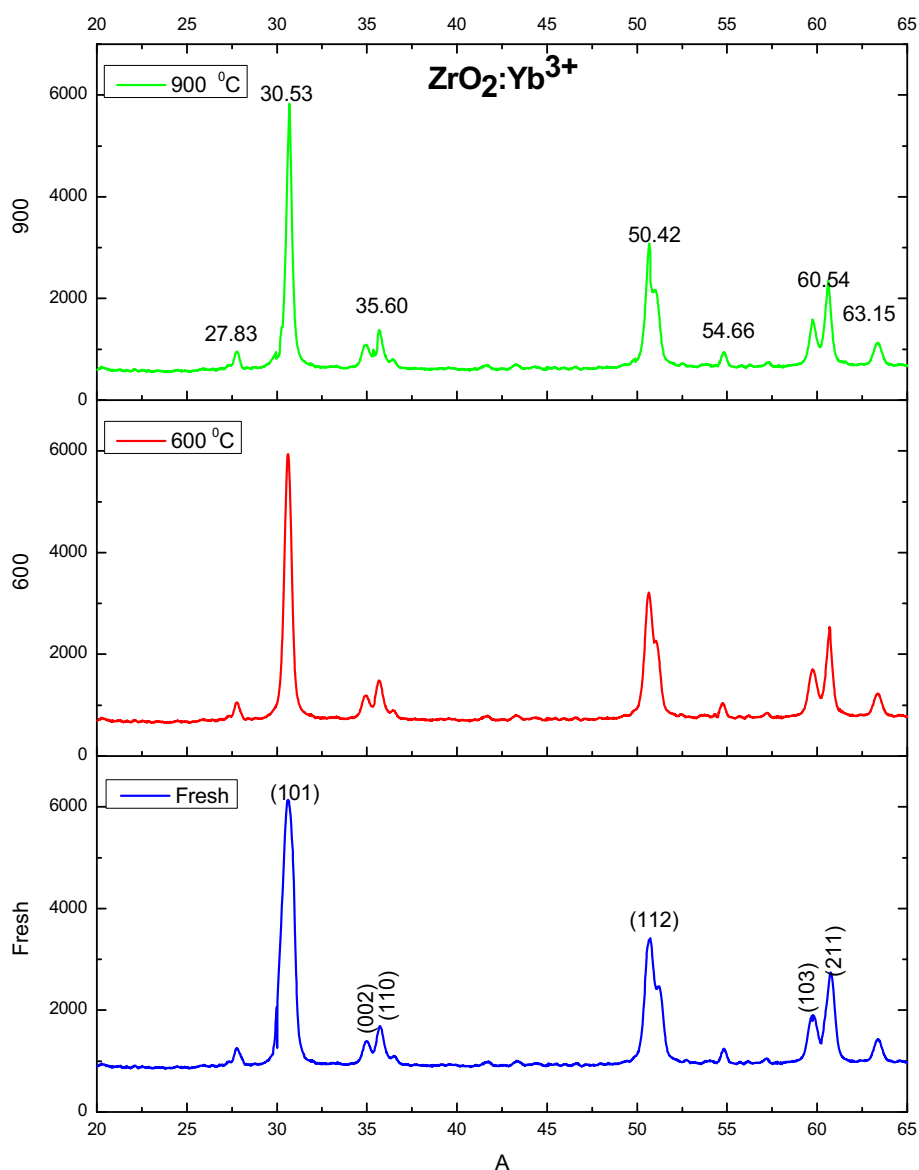


**Figure 1.** XRD results of ZrO<sub>2</sub>:Yb<sup>3+</sup> phosphor.

with annealing which confirms the increase in the crystal size with annealing of the sample. XRD patterns of  $\text{ZrO}_2:\text{Yb}^{3+}$ , in which seven different peaks were obtained at  $2\theta$  values of 27.83, 30.53, 35.60, 50.42, 54.66, 60.54 and 63.15°. The diffracted peaks show a major tetragonal phase, which is confirmed by the presence of a high intensity peak at  $2\theta$  values of 30.53 and 50.42° [13,14].

The size of the particles has been computed from the full width at half maximum (FWHM) of all the peaks using the Scherrer formula. The average crystal size was calculated using Scherrer's formula [15]. The Scherrer formula is given by:

$$D = \frac{K\lambda}{\beta \cos \theta},$$

where  $D$  is the average particle size perpendicular to the reflecting planes,  $K$  is the constant and the value is 0.89,

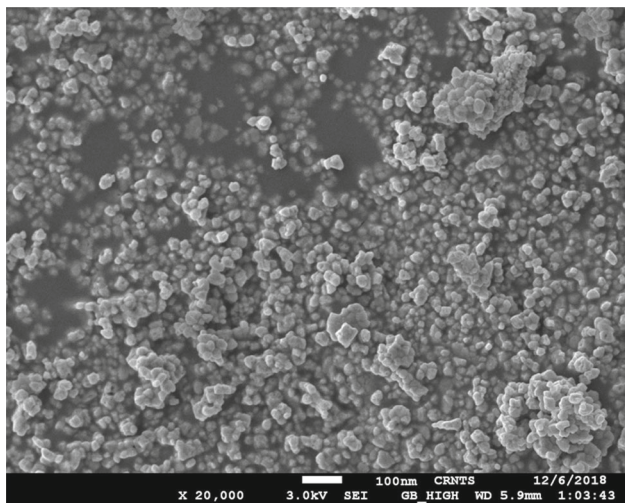


**Figure 2.** SEM results of  $\text{ZrO}_2:\text{Yb}^{3+}$  phosphor.

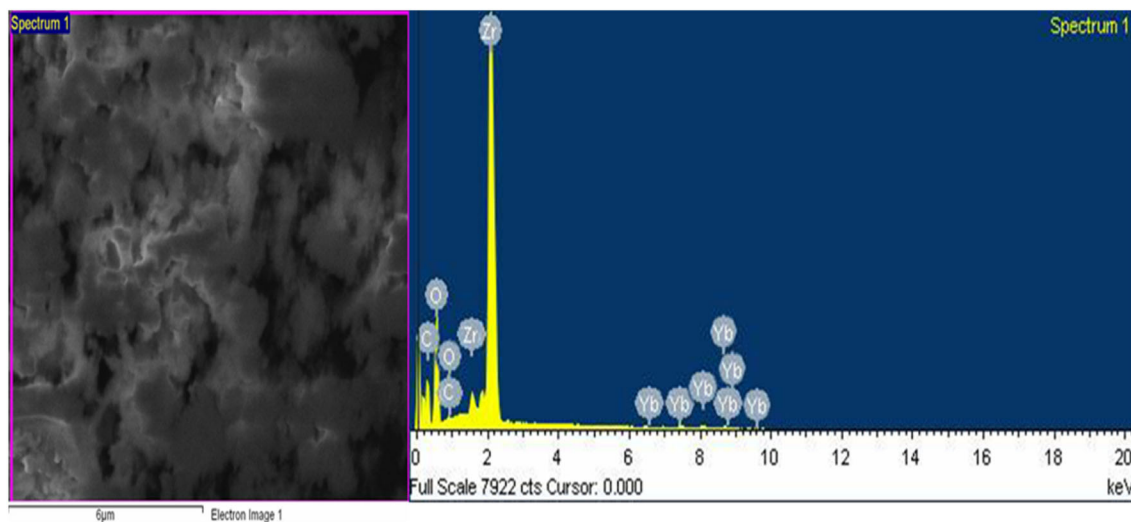


**Figure 3.** EDX spectra of  $\text{ZrO}_2:\text{Yb}^{3+}$  phosphor.

$\lambda$  is the X-ray wavelength,  $\beta$  is the FWHM and  $\theta$  is the diffraction angle. The average crystal size of the sample is found at around 22 nm.

### 3.2 Particle shape and size

The shape and size of the prepared nanocrystalline were determined by SEM. Figure 2 shows the SEM images of  $\text{ZrO}_2:\text{Yb}^{3+}$  phosphor nanoparticles produced by the chemical combustion technique.

### 3.3 EDX spectroscopy results

Combustion synthesized  $\text{ZrO}_2:\text{Yb}^{3+}$  phosphor was analysed by EDX analysis to obtain the chemical composition of the prepared phosphors. In the spectrum, intense peaks of Zr, Yb and O are present which confirm the formation of  $\text{ZrO}_2:\text{Yb}^{3+}$  phosphor (figure 3). The presence of C and Cu is due to the use of a carbon-coated copper grid in which the sample was placed for analysis. Quantitative elemental analysis of the prepared sample was also determined and the result is mentioned in table 1.

**Table 1.** Percentage elemental composition of the prepared phosphor.

Element	Weight%	Atomic%
C K	19.18	43.78
O K	24.26	39.62
Cu K	1.76	0.76
Zr L	50.70	15.24
Yb L	3.75	0.59
Total	100.00	—

#### 4. TL behaviour of Yb<sup>3+</sup>-doped ZrO<sub>2</sub> phosphor

The TL glow curve of Yb<sup>3+</sup>-doped ZrO<sub>2</sub> phosphor was recorded under 254 nm UV exposure. The TL glow curve was recorded for 5 min UV exposure at a heating rate of 6°C s<sup>-1</sup>. A single TL glow peak was found at 136°C for phosphor (figure 4).

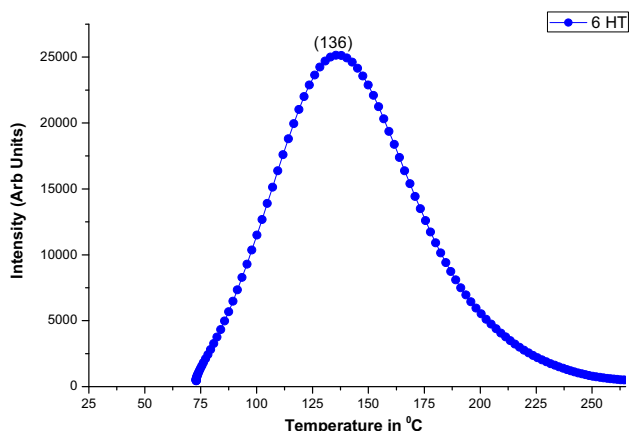


**Figure 4.** TL glow curve for freshly prepared Yb<sup>3+</sup>-doped ZrO<sub>2</sub> phosphors for fixed 5 min UV exposure at a heating rate of 6°C s<sup>-1</sup>.

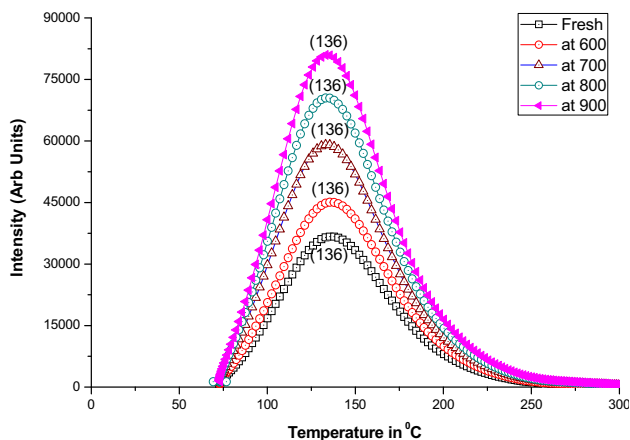


**Figure 5.** TL glow curve of Yb<sup>3+</sup>-doped ZrO<sub>2</sub> phosphor for fixed 5 min UV exposure at different annealing temperatures with a heating rate of 6°C s<sup>-1</sup>.

#### 4.1 Effect of annealing on Yb<sup>3+</sup>-doped ZrO<sub>2</sub> phosphors

To modify certain properties like crystal size, surface to volume ratio, etc., the prepared phosphor was annealed at different temperatures ranging from 600 to 900°C for 2 h. From the structural characterization of the sample, it was clear that as a result of annealing, the sample becomes free from internal stresses results in a refined and more homogeneous structure. The study of the TL glow curve at different annealing temperatures shows a continuous increase in the intensity of the TL glow peak (figure 5). This increase is the result of minimization of the residual TL signal at higher temperature [16]. The kinetic parameters were calculated for all the peaks obtained for different heating rates and are summarized in table 2. The activation energy for all the peaks has almost equivalent values which confirms that annealing of phosphor does not affect the formed traps and no new traps were formed as a result of annealing.

#### 4.2 Effect of different heating rates on Yb<sup>3+</sup> (1.5%)-doped ZrO<sub>2</sub> phosphors

To record the TL glow curve, the pre-irradiated sample is heated at a fixed rate. If the selected heating rate is low, the charge carriers have enough time to get retrapped, whereas at the higher heating rate, TL intensity diminishes due to the thermal quenching phenomenon [17,18]. Therefore, the optimization of heating rate to record the TL signal is a necessary process. To optimize the heating rate for UV exposed ZrO<sub>2</sub>:Yb<sup>3+</sup> phosphor, the TL glow curve was recorded at variable heating rates from 4 to 7°C s<sup>-1</sup> for fixed 5 min UV exposure. As the heating rate was increased from 4 to 6°C s<sup>-1</sup>, a slight increase in the peak intensity was observed with peak temperature shifting to the higher temperature side. However, with a further increase in the heating rate to 7°C s<sup>-1</sup>, the TL intensity again decreased and peak shifts towards higher temperature. Using the above results, the heating rate was optimized for 6°C s<sup>-1</sup> for both fresh and annealed samples (figures 6 and 7). Kinetic parameters were calculated to study the effect of the heating rate on traps for both fresh and annealed samples. The value of the activation energy for 6°C s<sup>-1</sup> has a minimum value which also confirms the optimization of this heating rate (tables 3 and 4).

**Table 2.** Kinetic parameters of Yb<sup>3+</sup>-doped ZrO<sub>2</sub> for fixed 5 min UV exposure at different annealing temperatures with a heating rate of 6°C s<sup>-1</sup>.

Annealing temperature (°C)	T <sub>1</sub> (°C)	T <sub>m</sub> (°C)	T <sub>2</sub> (°C)	τ	δ	ω	μ = δ/ω	Activation energy, E (eV)	Frequency factor, S (s <sup>-1</sup> )
Fresh	102	136	176	34	40	74	0.541	0.644	1.1 × 10 <sup>9</sup>
600	104	136	177	32	41	73	0.562	0.69	4.2 × 10 <sup>9</sup>
700	103	136	176	33	40	73	0.548	0.656	1.8 × 10 <sup>9</sup>
800	102	136	175	34	39	73	0.534	0.634	9.5 × 10 <sup>8</sup>
900	103	136	176	33	40	73	0.548	0.656	1.8 × 10 <sup>9</sup>

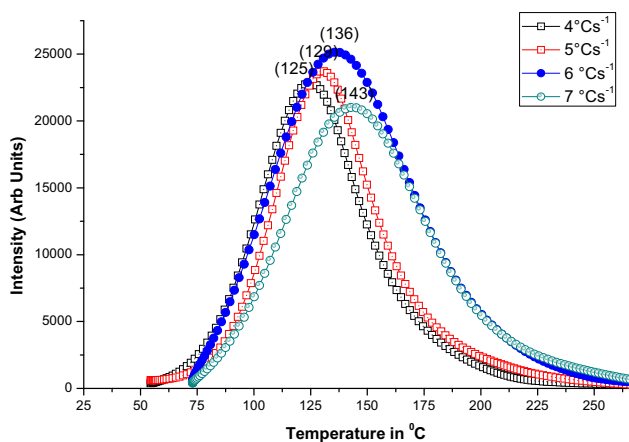


**Figure 6.** TL glow curve at different heating rates for freshly prepared  $\text{Yb}^{3+}$ -doped  $\text{ZrO}_2$  phosphors for fixed 5 min UV exposure.

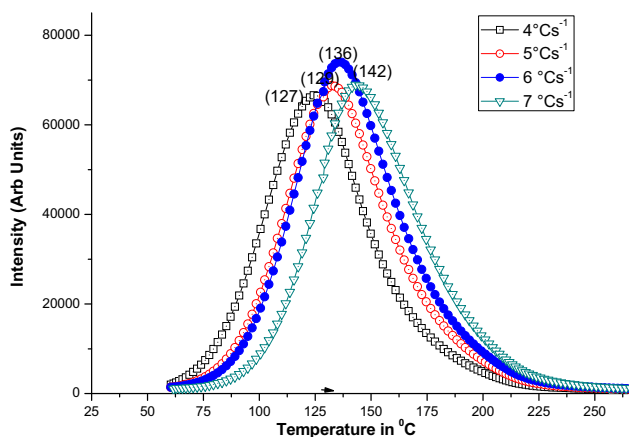


**Figure 7.** TL glow curve of  $\text{Yb}^{3+}$ -doped  $\text{ZrO}_2$  phosphor annealed at  $900^\circ\text{C}$  for different heating rates.

### 4.3 Effect of UV exposure time on $\text{Yb}^{3+}$ (1.5%)-doped $\text{ZrO}_2$ phosphors

The TL glow curves of  $\text{Yb}^{3+}$ -doped  $\text{Gd}_2\text{O}_3$  phosphor with the variation of the UV exposure time have been recorded. The TL response in terms of intensity (peak intensity of the TL glow curve) is found to be continuously increasing from 5 to 25 min

UV exposure, then it starts to decrease (figure 8). This wide response is an extraordinary result obtained not only for this phosphor, but also for many nanostructure materials [19]. The activation energy for different UV exposure times has almost the same value which confirms that the UV radiation does not affect the position of trap levels (table 5).

### 4.4 Effect of $\text{Yb}^{3+}$ concentration

Effects of different concentrations of  $\text{Yb}^{3+}$  from 1 to 7 mol % on the TL response of  $\text{ZrO}_2:\text{Yb}^{3+}$  nanophosphors were studied (figure 9). For this, the TL glow curves with the variable concentrations of  $\text{Yb}^{3+}$  (1–7 mol%) were recorded for constant UV exposure of 25 min and at constant heating rate of  $6^\circ\text{C s}^{-1}$ . It was noticed that the integrated area of the curve for UV exposure increases with increasing  $\text{Yb}^{3+}$  concentration up to 4 mol%. Furthermore, the glow peak structure remains the same for all the concentrations of  $\text{Yb}^{3+}$ , however, the TL intensity varies with  $\text{Yb}^{3+}$  concentration. The intensity of the TL glow curve increases with an increase in the dopant concentration ( $\text{Yb}^{3+}$ ) up to 4 mol% of  $\text{Yb}^{3+}$  and then, the TL intensity decreases further with an increase in  $\text{Yb}^{3+}$  concentration. This decrease in TL intensity is due to the concentration quenching which destroys trap levels. Kinetic parameters are presented in table 6.

**4.4a CGCD:** The trapping parameters of localized energy levels within the crystal and defects in the phosphor have been determined by using the computerized glow curve deconvolution (CGCD). It helps in better understanding of the TL mechanism. By considering this fact, the CGCD curve fitting was performed by using a glow curve deconvolution function applied on the obtained glow curve under optimized conditions to isolate each peak [18]. The deconvoluted curve has three peaks at 104, 133 and  $168^\circ\text{C}$ . The activation energy, order of kinetics and frequency factor for each peak are calculated and summarized in table 7. The activation energies corresponding to peaks at 104, 133 and  $168^\circ\text{C}$  were found to be 0.96, 0.83 and 0.63 eV, respectively (figure 10).

**4.4b Probable model to explain concentration quenching in TL behaviour of  $\text{ZrO}_2:\text{Yb}^{3+}$  phosphor:** Theoretically, the TL peak at higher temperature should have higher activation energy than the lower temperature peak, but in the

**Table 3.** Kinetic parameters at different heating rates for freshly prepared  $\text{Yb}^{3+}$  (1.5)-doped  $\text{ZrO}_2$  phosphors for fixed 5 min UV exposure.

Heating rate	$T_1$ ( $^\circ\text{C}$ )	$T_m$ ( $^\circ\text{C}$ )	$T_2$ ( $^\circ\text{C}$ )	$\tau$	$\delta$	$\omega$	$\mu = \delta/\omega$	Activation energy, $E$ (eV)	Frequency factor, $S$ ( $\text{s}^{-1}$ )
4	98	125	151	27	26	53	0.491	0.758	$6.1 \times 10^{10}$
5	104	129	157	25	28	53	0.528	0.844	$6.4 \times 10^{11}$
6	102	136	175	34	39	73	0.534	0.643	$1.2 \times 10^9$
7	109	143	180	34	37	71	0.521	0.662	$1.3 \times 10^9$

**Table 4.** Kinetic parameters of Yb<sup>3+</sup>-doped ZrO<sub>2</sub> phosphor annealed at 900°C for different heating rates.

Heating rate	T <sub>1</sub> (°C)	T <sub>m</sub> (°C)	T <sub>2</sub> (°C)	τ	δ	ω	μ = δ/ω	Activation energy, E (eV)	Frequency factor, S (s <sup>-1</sup> )
4	100	127	153	27	26	53	0.491	0.766	6.8 × 10 <sup>10</sup>
5	104	129	157	25	28	53	0.528	0.844	6.4 × 10 <sup>11</sup>
6	100	133	173	33	40	73	0.548	0.656	1.8 × 10 <sup>9</sup>
7	109	142	182	33	40	73	0.548	0.685	1.7 × 10 <sup>9</sup>

present result, the peak at higher temperature i.e., 168°C has relatively lower activation energy. As the present work deals with the tuning of the TL behaviour of ZrO<sub>2</sub>:Yb<sup>3+</sup> phosphor with dopant concentration, we proposed a model to explain the effect of the concentration quenching on the dopant concentration. To explain the effect of concentration quenching the energy level model with three traps and one recombination centre (3T1R) is used here [20,21] (figure 11).

According to this model, there are three electron traps with concentrations φ<sub>1</sub>, φ<sub>2</sub>, φ<sub>3</sub> and φ<sub>1</sub>, φ<sub>2</sub>, φ<sub>3</sub> are the respective instantaneous occupancies. ε<sub>1</sub>, ε<sub>2</sub> and ε<sub>3</sub> are the respective activation energies; f<sub>1</sub>, f<sub>2</sub> and f<sub>3</sub> are the respective frequency factors and P<sub>1</sub>, P<sub>2</sub> and P<sub>3</sub> are the corresponding retrapping probability coefficient for trap1, trap2 and

trap3, respectively. M represents the concentration of the recombination centre and m is the instantaneous occupancy of the holes and the probability coefficient for the hole to be trapped in the recombination centre is β. P<sub>m</sub> is the electron recombination probability coefficient, C<sub>B</sub> and V<sub>B</sub> are the concentrations of free electrons and holes, respectively. The excitation dose responsible for the electron-hole pair is represented by X. The concentration of the recombination centre M is variable with variation in the dopant concentration in different samples, whereas the other concentrations of the traps are considered to be constant. The excitation dose is also kept constant during simulation of the excitation of the different samples containing different concentrations of dopants. The governing process during

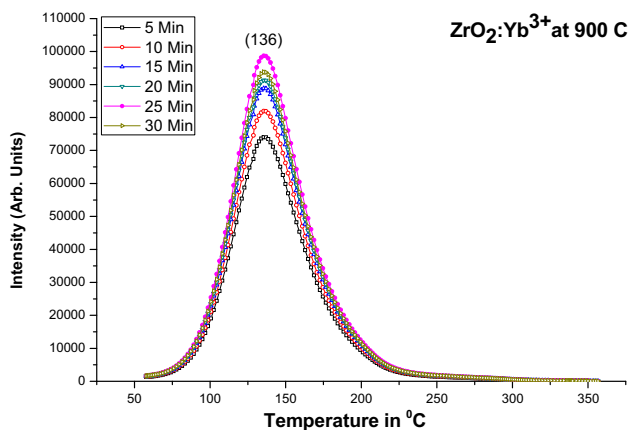


**Figure 8.** TL glow curve intensities for Yb<sup>3+</sup>-doped ZrO<sub>2</sub> phosphors for different UV exposure times with a heating rate of 6°C s<sup>-1</sup>.

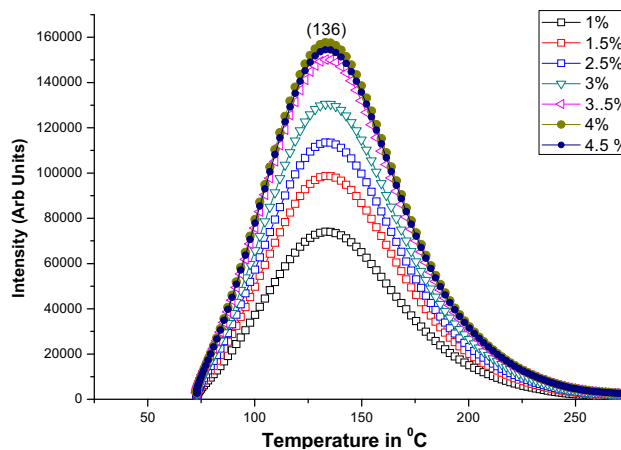


**Figure 9.** TL glow curve of Yb<sup>3+</sup>-doped ZrO<sub>2</sub> (0.5–4.5%) phosphor annealed at 900°C for a heating rate of 6°C.

**Table 5.** Kinetic parameters of Yb<sup>3+</sup> (1.5%)-doped ZrO<sub>2</sub> phosphors for different UV exposure times with a heating rate of 6°C s<sup>-1</sup>.

UV exposure time	T <sub>1</sub> (°C)	T <sub>m</sub> (°C)	T <sub>2</sub> (°C)	τ	δ	ω	μ = δ/ω	Activation energy, E (eV)	Frequency factor, S (s <sup>-1</sup> )
5	102	136	180	34	44	78	0.564	0.65	1.2 × 10 <sup>9</sup>
10	101	136	175	35	39	74	0.527	0.623	5.7 × 10 <sup>8</sup>
15	100	136	175	36	39	75	0.52	0.604	3.2 × 10 <sup>8</sup>
20	102	136	174	34	38	72	0.528	0.641	1.4 × 10 <sup>9</sup>
25	102	136	176	34	40	74	0.541	0.644	1.0 × 10 <sup>9</sup>
30	101	136	175	35	39	74	0.527	0.623	5.7 × 10 <sup>8</sup>

**Table 6.** Kinetic parameters of Yb<sup>3+</sup> (0.5–4.5%)-doped ZrO<sub>2</sub> phosphor annealed at 900°C for a heating rate of 6°C.

Yb <sup>3+</sup> concentration	T <sub>1</sub> (°C)	T <sub>m</sub> (°C)	T <sub>2</sub> (°C)	τ	δ	ω	μ = δ/ω	Activation energy, E (eV)	Frequency factor, S (s <sup>-1</sup> )
0.5	100	133	173	33	40	73	0.548	0.656	1.7 × 10 <sup>9</sup>
1	100	133	173	33	40	73	0.548	0.656	1.7 × 10 <sup>9</sup>
1.5	102	133	173	31	40	71	0.563	0.702	7.1 × 10 <sup>9</sup>
2	100	133	172	33	39	72	0.542	0.654	1.7 × 10 <sup>9</sup>
2.5	99	133	171	34	38	72	0.528	0.632	8.7 × 10 <sup>8</sup>
3	101	133	170	32	37	69	0.536	0.674	3.0 × 10 <sup>9</sup>
4	100	133	171	33	38	71	0.535	0.653	1.6 × 10 <sup>9</sup>
4.5	101	133	171	32	38	70	0.543	0.675	3.2 × 10 <sup>9</sup>

**Table 7.** Kinetic parameters calculated for the deconvoluted curve.

Peaks	T <sub>1</sub> (°C)	T <sub>m</sub> (°C)	T <sub>2</sub> (°C)	μ <sub>g</sub>	E (eV)	S (s <sup>-1</sup> )
1	85.6	104.8	123.5	0.4934	0.9636	1.5 × 10 <sup>14</sup>
2	107.12	133	161.53	0.5244	0.8304	3.4 × 10 <sup>11</sup>
3	128.3	168.5	209.2	0.5031	0.6263	1.4 × 10 <sup>8</sup>

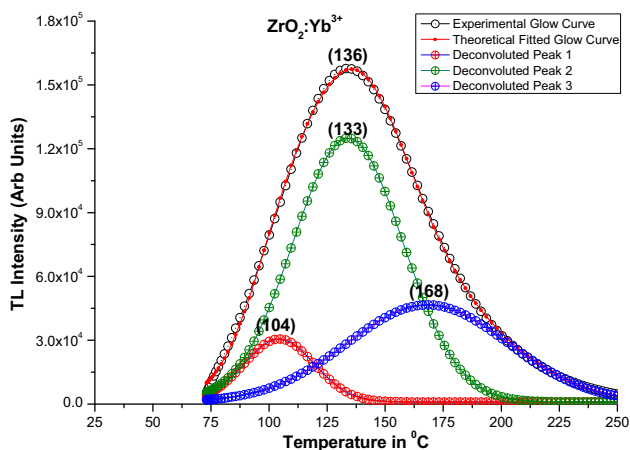


**Figure 10.** Deconvoluted TL spectra of Yb<sup>3+</sup>-doped ZrO<sub>2</sub> phosphor under optimum conditions.

excitation can be represented by the following differential equations:

$$\frac{d\phi'_1}{dt} = P_1(\phi_1 - \phi'_1)C_B, \tag{1}$$

$$\frac{d\phi'_2}{dt} = P_2(\phi_2 - \phi'_2)C_B, \tag{2}$$

$$\frac{d\phi'_3}{dt} = P_3(\phi_3 - \phi'_3)C_B, \tag{3}$$

$$\frac{dm}{dt} = \beta(M - m)n_v - P_m m C_B, \tag{4}$$

$$\frac{dV_B}{dt} = X - \beta(M - m)V_B, \tag{5}$$

$$\frac{dC_B}{dt} = \frac{dm}{dt} + \frac{dV_B}{dt} - \frac{d\phi'_1}{dt} - \frac{d\phi'_2}{dt} - \frac{d\phi'_3}{dt}. \tag{6}$$

Experimental values have been determined by solving the above mentioned equations with respect to time *t*. The excitation dose is proportional to *X*<sub>1</sub>. Excitation is followed by the relaxation containing electrons and holes present in the conduction and valance bands, respectively, which undergoes retrapping by decaying the respective traps. Retrapping of e<sup>-</sup> and holes results in the TL signals as a function of the TL signal under the influence of heat energy. The following equations are obtained by solving the above mentioned equations:

$$\frac{d\phi'_1}{dt} = P_1(\phi_1 - \phi'_1)C_B - S_1\phi'_1 \exp(-\varepsilon_1/kT), \tag{7}$$

$$\frac{d\phi'_2}{dt} = P_2(\phi_2 - \phi'_2)C_B - S_2\phi'_2 \exp(-\varepsilon_2/kT), \tag{8}$$

$$\frac{d\phi'_3}{dt} = P_3(\phi_3 - \phi'_3)C_B - S_3\phi'_3 \exp(-\varepsilon_3/kT), \tag{9}$$

$$\frac{dm}{dt} = -P_m m C_B, \tag{10}$$

$$\frac{dC_B}{dt} = \frac{dm}{dt} - \frac{d\phi'_1}{dt} - \frac{d\phi'_2}{dt} - \frac{d\phi'_3}{dt}. \tag{11}$$

The TL intensity as a function of temperature (*T*) can be written as:

$$I(T) = -\frac{dm}{dt} = P_m m C_B. \tag{12}$$

The differential equations were solved numerically by applying simulation at all the stages involved in the TL process. The numerical values for the parameters in the model are:  $\phi'_1 = 2.99 \times 10^8 \text{ cm}^{-3}$ ,  $\phi'_2 = 0.98 \times 10^7 \text{ cm}^{-3}$ ,  $\phi'_3 = 2.01 \times 10^{-9}$ ,  $P_1 = 1 \times 10^{-8} \text{ cm}^3 \text{ s}^{-1}$ ,  $P_2 = 1 \times 10^{-8} \text{ cm}^3 \text{ s}^{-1}$ ,  $P_3 = 1 \times 10^{-9} \text{ cm}^3 \text{ s}^{-1}$ ,  $P_m = 1 \times 10^{-10} \text{ cm}^3 \text{ s}^{-1}$ ,  $\beta = 1 \times$

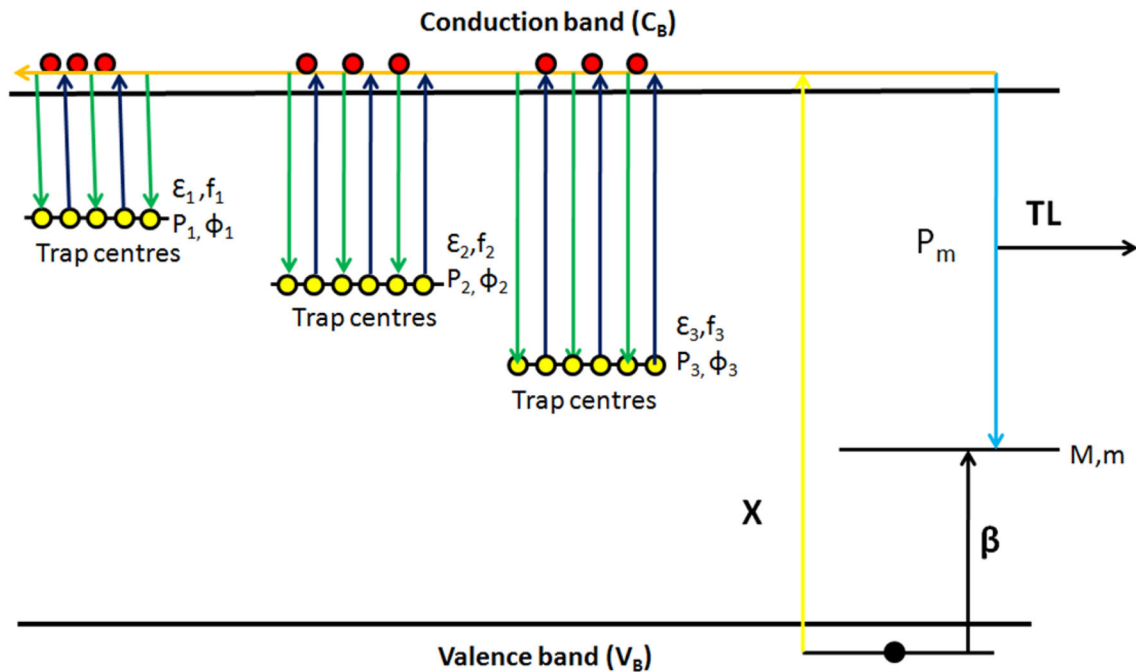


Figure 11. Energy level diagram of the three trap one recombination centre model.

$10^{-9} \text{ cm}^3 \text{ s}^{-1}$ ,  $\epsilon_1 = 0.96 \text{ eV}$ ,  $\epsilon_2 = 0.83 \text{ eV}$ ,  $\epsilon_3 = 0.62 \text{ eV}$ ,  $f_1 = 1.5 \times 10^{14} \text{ s}^{-1}$ ,  $f_2 = 3.4 \times 10^{11} \text{ s}^{-1}$ ,  $f_3 = 1.4 \times 10^8 \text{ s}^{-1}$ ,  $D = 5 \times 10^7 \text{ cm}^{-3}$  and  $\beta = 6^\circ\text{C s}^{-1}$ .

During the excitation stage, the initial occupancy of the recombination centre was chosen as 0.1  $M$ . The simulation results show that the two TL glow peaks reach maxima at different concentrations [22,23].

To explain the effect of concentration quenching, the model was analysed. During the analysis of the proposed model, it was considered that all the traps  $\phi_1$ ,  $\phi_2$  and  $\phi_3$  were fixed and the recombination centre  $M$  was varied. The initial instantaneous occupancies  $\Phi'_1 = \Phi'_2 = \Phi'_3 = 0$  and  $m = \alpha M$ , here, the value of  $\alpha$  was determined by Fermi statistics. The value of  $\alpha$  remains constant for variable concentration of  $M$ . The dose provided to the sample was not enough for the saturation of traps, therefore,  $\Phi_1 \ll \phi_1$ ,  $\Phi_2 \ll \phi_2$  and  $\Phi_3 \ll \phi_3$ . The radiation dose  $D$  was provided to the sample and is equal to  $X_1$ . After dose  $D$ , the population concentrations  $n_1$  and  $n_2$  of electron–hole pairs can be represented by the following equations:

$$\Phi_1 = \frac{P_1\phi_1}{P_1\phi_1 + P_2\phi_2 + P_3\phi_3 + P_m\alpha M} D, \tag{13}$$

$$\Phi_2 = \frac{P_2\phi_2}{P_1\phi_1 + P_2\phi_2 + P_3\phi_3 + P_m\alpha M} D. \tag{14}$$

At the time of TL measurement, initially the electron from the first trap  $\phi_1$  excited to the conduction band and subsequently trapped by either second or third trap levels  $\phi_2$  and  $\phi_3$  or recombination centre  $M$ . The retrapping of the electron by

the recombination centre  $M$  is responsible for TL emission. The integrated intensity of the first TL peak is approximately,

$$I_{1,\text{int}} = \frac{P_m\alpha M}{P_2\phi_2 + P_3\phi_3 + P_m\alpha M} \Phi_1 \frac{P_m\alpha M}{P_2\phi_2 + P_3\phi_3 + P_m\alpha M} \times \frac{P_1\phi_1}{P_1\phi_1 + P_2\phi_2 + P_3\phi_3 + P_m\alpha M} D. \tag{15}$$

For a small dopant concentration,  $M$  has a smaller value,  $P_m\alpha M \ll P_2\phi_2 + P_3\phi_3$ , so that  $P_m\alpha M$  can be neglected in the denominator and the TL intensity becomes directly proportional to  $M$  i.e., the TL increases linearly with increasing  $M$ . As the dopant concentration increases, the value of  $M$  also increases which results in  $P_m\alpha M \gg P_1\phi_1 + P_2\phi_2 + P_3\phi_3$ , so that the denominator grows as the squares of  $M$  and the TL intensity decreases with an increase in  $M$ . Thus, initially the TL intensity grows with an increase in the concentration of  $M$ , then, it levels off and then decreases with a further increase in  $M$  concentration. During excitation of  $\Phi_1$ , some of the electrons were trapped by  $\phi_2$ . Due to this, the population concentration  $\Phi_2$  changes. The change in  $\Phi_2$  can be represented as:

$$\Delta\Phi_2 = \frac{P_2\phi_2}{P_2\phi_2 + P_3\phi_3 + P_m\alpha M} \Phi_1, \tag{16}$$

$$\Delta\Phi_2 = \frac{P_2\phi_2}{P_2\phi_2 + P_3\phi_3 + P_m\alpha M} \times \frac{P_1\phi_1}{P_1\phi_1 + P_2\phi_2 + P_3\phi_3 + P_m\alpha M} D. \tag{17}$$



The total concentration  $\Phi'_2$  is:

$$\Phi'_2 = \frac{P_2\phi_2}{P_1\phi_1 + P_2\phi_2 + P_3\phi_3 + P_m\alpha M} \times \left(1 + \frac{P_1\phi_1}{P_2\phi_2 + P_3\phi_3 + P_m\alpha M}\right) D, \quad (18)$$

$$\Phi'_2 = \frac{P_2\phi_2}{P_2\phi_2 + P_3\phi_3 + P_m\alpha M} D. \quad (19)$$

The changes in  $\Phi_3$  and  $m$  during this step is negligible. As the temperature increases continuously, the electron  $\Phi'_2$  retrapped by the second trap  $\phi_2$ , becomes free and are captured by either  $\phi_3$  or  $M$ . The integrated intensity of the second peak is represented as:

$$I_{2,\text{int}} = \frac{P_m\alpha M}{P_2\phi_2 + P_3\phi_3 + P_m\alpha M} \Phi'_2, \quad (20)$$

$$I_{2,\text{int}} = \frac{P_m\alpha M}{P_3\phi_3 + P_m\alpha M} \times \frac{P_2\phi_2}{P_2\phi_2 + P_3\phi_3 + P_m\alpha M} D. \quad (21)$$

The intensity increases linearly for the smaller value of  $M$  due to:

$$P_m\alpha M \ll P_3\phi_3.$$

And the intensity shows inverse relation at higher  $M$  concentration due to:

$$P_m\alpha M \gg P_2\phi_2 + P_3\phi_3.$$

The value of  $P_m\alpha M$  indicates that  $I_1$  and  $I_2$  will peak at different values of  $M$ . With an increase in the value of  $M$ , the first peak reaches the maxima before the second peak. It is due to competition in trapping among the three traps during excitation and read out time.

## 5. Conclusion

$\text{Yb}^{3+}$ -doped  $\text{ZrO}_2$  was synthesized by the combustion synthesis method. The prepared phosphor has a cubic phase, which was confirmed by the XRD pattern of phosphor. The crystal size was found at around 22 nm. The TL glow curve was recorded under 254 nm UV excitation. The optimized conditions for the TL glow curve are: heating rate of  $6^\circ\text{C s}^{-1}$ , UV exposure time of 25 min and  $\text{Yb}^{3+}$  concentration of 4 mol%. The CGCD was applied for the TL glow curve obtained for the optimized curve. The CGCD curve has three peaks which show the formation of three traps. Kinetic parameters for each

condition were calculated and the maximum parameters do not affect the values of activation energy which confirms that they do not affect the formed traps. Three trap one recombination centre model was used to explain the concentration quenching behaviour of the prepared phosphor.

## References

- [1] Shoaib K A, Hashmi F H, Ali M, Bukhari S J H and Majid C A 1997 *Phys. Status Solidi A* **40** 605
- [2] Mukherjee B, Lambert J, Hentschel R, Negodin E and Farr J 2011 *Radiat. Meas.* **46** 1698
- [3] Laopaiboon R and Bootjomchai C 2015 *J. Lumin.* **158** 275
- [4] Chowdhury M, Sharma S K and Lochab S P 2016 *Ceram. Int.* **42** 5472
- [5] Malleshappa J, Nagabhushana H, Prasad B D, Sharma SC, Vidya Y S and Anantharaju K S 2016 *Optik—Int. J. Light Electron Opt.* **127** 855
- [6] Rivera T, Azorín J, Falcony G, García M and Martínez E 2002 *Radiat. Prot. Dosim.* **100** 317
- [7] Salas P, De la Rosa-Cruz E, Díaz-Torres L A, Castaño V M, Melendrez R and Barboza-Flores M 2003 *Radiat. Meas.* **37** 187
- [8] Montalvo T R, Tenorio L, Nieto J A, Salgado M B, Estrada M S and Furetta C 2005 *Radiat. Eff. Defects Solids* **160** 181
- [9] Villa-Sánchez G, Mendoza-Anaya D, Eufemia Fernández-García M, Escobar-Alarcón L, Olea-Mejía O and González-Martínez P R 2014 *Opt. Mater.* **36** 1219
- [10] Rivera T, Olvera L, Azorín J, Sosa R, Barrera M, Soto A M et al 2006 *Radiat. Eff. Defects Solids* **161** 91
- [11] Villa-Sánchez G, Mendoza-Anaya D, Mondragón-Galicia G, Pérez-Hernández R, Olea-Mejía O and González Martínez P R 2014 *Radiat. Phys. Chem.* **97** 118
- [12] Zhang Y W, Sun X, Xu G and Yan C H 2004 *Solid State Sci.* **6** 523
- [13] Aruna S T and Rajam K S 2004 *Mater. Res. Bull.* **39** 157
- [14] Salah N, Habib S S, Khan Z H and Djouider F 2011 *Radiat. Phys. Chem.* **80** 923
- [15] Guinier A 1963 *X-ray diffraction in crystals, imperfect crystals, and amorphous bodies* (San Francisco: Freeman) ISBN No.: 9780486141343
- [16] Horowitz Y S 1984 (USA: CRC Press) p 89
- [17] Gokce M, Oguz K F, Karali T and Prokic M 2009 *J. Phys. D: Appl. Phys.* **42** 105412
- [18] Bahl S, Pandey A, Lochab S P, Aleynikov V E, Molokanov A G and Kumar P 2013 *J. Lumin.* **134** 691
- [19] Sunitha D V, Shivakumara C and Chakradhar R P S 2012 *Spectrochim. Acta, Part A* **96** 532
- [20] Chen R, Lawless J L and Pagonis V 2011 *Radiat. Meas.* **46** 1380
- [21] Tamrakar R K, Upadhyay K and Bisen D P 2017 *Phys. Chem. Chem. Phys.* **19** 14680
- [22] Lochab S P, Pandey A, Sahare P D, Chauhan R S, Salah N and Ranjan R 2007 *Phys. Status Solidi A* **204** 2416
- [23] Singh L, Chopra V and Lochab S P 2011 *J. Lumin.* **131** 1177